

THE CLUSTER SUBSTRUCTURE - ALIGNMENT CONNECTION

Manolis Plionis

*Institute of Astronomy & Astrophysics, National Observatory of Athens, I.Metaxa & B.Pavlou,
P.Penteli, 152 36 Athens, Greece*

Using the APM cluster data we investigate whether the dynamical status of clusters is related to the large-scale structure of the Universe. Due to difficulties in determining unambiguously the dynamical status of clusters in optical data, our substructure identification method has been calibrated using jointly ROSAT X-ray and optical data for a subsample of 22 Abell clusters. We find that cluster substructure is strongly correlated with the tendency of clusters to be aligned with their nearest neighbour and in general with the nearby clusters that belong to the same supercluster. Furthermore, dynamically young clusters are more clustered than the overall cluster population. These are strong indications that cluster develop in a hierarchical fashion by anisotropy merging along the large-scale filamentary superclusters within which they are embedded.

1 Overview

Galaxy clusters occupy a special position in the hierarchy of cosmic structure in many respects. Being the largest bound structures in the universe, they contain hundreds of galaxies and hot X-ray emitting gas and thus can be detected at large redshifts. Therefore, they appear to be ideal tools for studying large-scale structure, testing theories of structure formation and extracting invaluable cosmological information (cf. Böhringer⁸, Schindler³⁵, Borgani & Guzzo⁷).

Below I will review a few issues related to cluster dynamics and the cluster large-scale environment. Using the APM cluster catalogue (Dalton *et al*¹⁰) and methods calibrated using both optical and X-ray data I will present significant evidence that the cluster internal structure and dynamical state is strongly related to their large-scale distribution.

This contribution is based on different works which are in preparation with collaborators of different parts of the project being S.Basilakos, S.Maurocordato, E.Slezak, C.Benoist and others.

1.1 Cluster Internal Dynamics & Cosmology

One of the interesting properties of galaxy clusters is the relation between their dynamical state and the underlying cosmology. Although the physics of cluster formation is complicated (cf. Sarazin³³), it is expected that in an open or a flat with vacuum-energy contribution universe, clustering effectively freezes at high redshifts ($z \simeq \Omega_m^{-1} - 1$) and thus clusters today should appear more relaxed with weak or no indications of substructure. Instead, in a critical density model, such systems continue to form even today and should appear to be dynamically active (cf. Richstone, Loeb & Turner²⁷, Evrard *et al.*¹³, Lacey & Cole²⁰). Using the above theoretical expectations as a cosmological tool is hampered by two facts:

- ⊙ *Ambiguity in identifying cluster substructure:* One has to deal with the issue of unambiguously identifying cluster substructure, since projection effects in the optical can conspire to make cluster images appear having multiple peaks/substructure. A lot of work has been devoted in attempts to find criteria and methods to identify cluster substructure (see references in Kolokotronis *et al*¹⁹). It is evident from all the available studies that there is neither agreement on the methods utilised nor on the exact frequency of clusters having substructure.
- ⊙ *Unknown physics of cluster merging:* The clear-cut theoretical expectations regarding the fraction of clusters expected to be relaxed in different cosmological backgrounds breakdown due to the complicated physics of cluster merging (cf. Sarazin³³) and especially due to the uncertainty of the post-merging relaxation time. In other words, identifying a cluster with significant substructure does not necessarily mean that this cluster is dynamically young, but could reflect an ancient merging that has not relaxed yet to an equilibrium configuration.

Mohr *et al.*²², Rizza *et al.*²⁸ and Kolokotronis *et al.*¹⁹ have investigated the frequency of cluster substructure using in a complementary fashion optical and X-ray data. The advantage of using X-ray data is that the X-ray emission is proportional to the square of the gas density (rather than just density in the optical) and therefore it is centrally concentrated, a fact which minimises projection effects (cf. Sarazin³², Schindler³⁴). The advantage of using optical data is the sheer size of the available cluster catalogues and thus the statistical significance of the emanating results. Kolokotronis *et al*¹⁹ calibrated various substructure measures using APM and ROSAT data of 22 Abell clusters and found that in most cases using X-ray or optical data one can identify substructure unambiguously. Only in $\sim 20\%$ of the clusters they studied did they find projection effects in the optical that altered the X-ray definition of substructure. Their conclusion was that solely optical cluster imaging data can be used in order to identify the clusters that have significant substructure.

However, as we discussed previously, it seems that in order to take advantage of the different rates of cluster evolution in the different cosmological backgrounds one needs (a) to find criteria of recent cluster merging and (b) calibrate the results using high-resolution cosmological hydro simulation, which will provide the expectations of the different cosmological models.

Such criteria have been born out of numerical simulations (cf. Roettiger *et al.*^{29 30}) and are based on the use of multiwavelength data, especially optical and X-ray data but radio as well (cf. Zabludoff & Zaritsky⁴⁴, Schindler³⁴, Sarazin, in this volume). The criteria are based on the fact that gas is collisional while galaxies are not and therefore during the merger of two clumps, containing galaxies and gas, we expect: (1) a difference in the spatial positions of the highest peak in the galaxy and gas distribution, (2) the X-ray emitting gas, due to compression along the merging direction, to be elongated perpendicularly along this direction and (3) temperature gradients to develop due to the compression and subsequent shock heating of the gas.

Figure 1 presents the smoothed optical (APM) and X-ray (ROSAT pointed observations) density distributions of 4 Abell clusters, out of which 3 show such evidence of recent merging, while A2580 seems to be in a relaxed state (for details of the smoothing procedure see Kolokotronis *et al*¹⁹). Note that BeppoSAX observations of Abell 3266 (de Grandi & Molendi¹²) has shown the existence of a temperature gradient dropping from 10 keV in the cluster core to 5 keV at about 1.5 Mpc distance, consistent with a merging event, a fact which is also apparent, in figure 1, from the comparison of the optical and X-ray image of the cluster.

1.2 Cluster Alignments and Formation Processes

Another interesting observable, that was thought initially to provide strong constraints on theories of galaxy formation, is the tendency of clusters to be aligned with their nearest neighbour

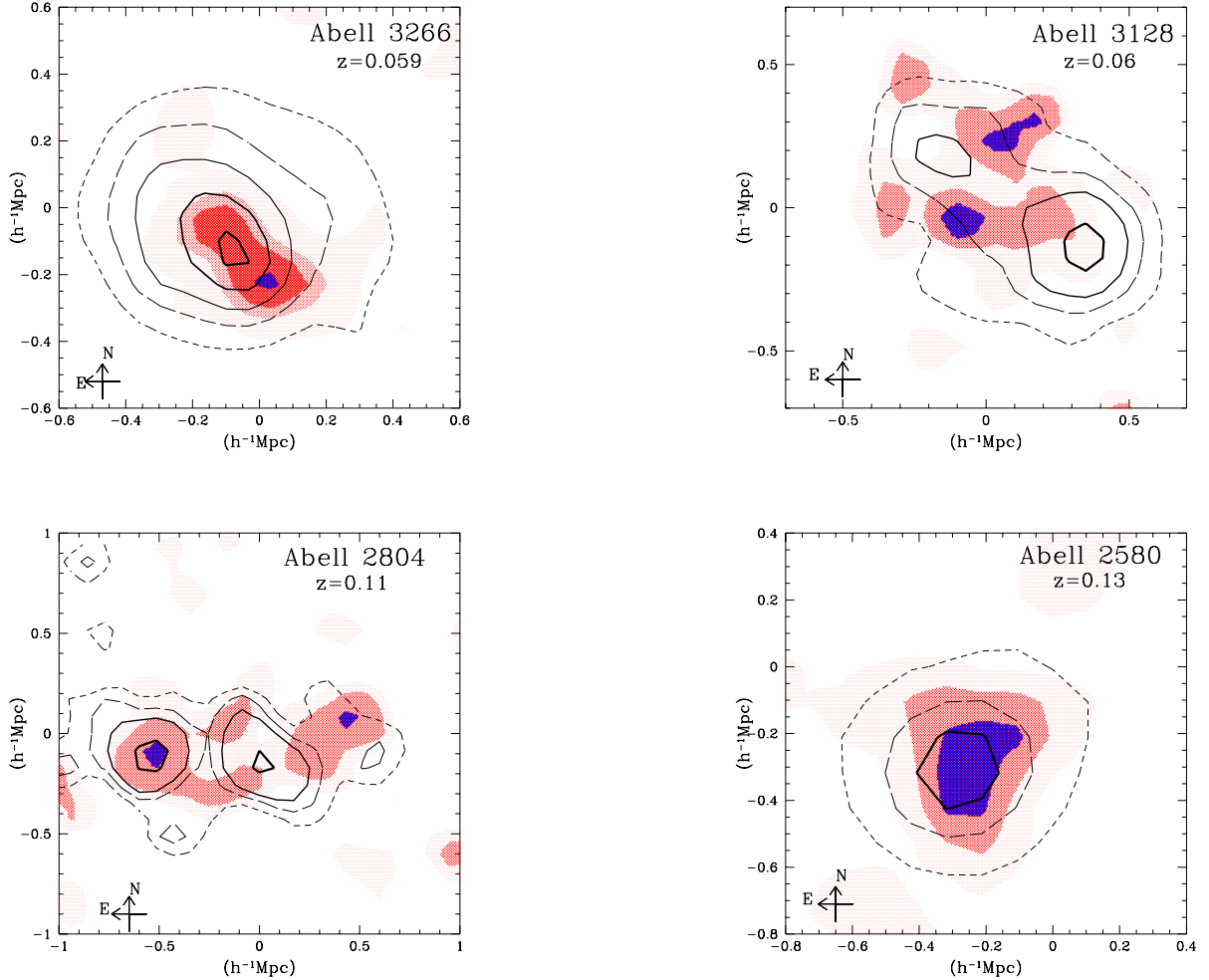


Figure 1: Optical APM (colour) and ROSAT Xray (contour) images of 4 Abell clusters. Peaks of the APM galaxy distribution is shown in blue. Note that apart from A2804, the rest are HRI images.

as well as with other clusters that reside in the same supercluster (cf. Binggeli⁴, West⁴⁰, Plionis²⁶). Analytical work of Bond^{5 6} in which clusters were identified as peaks of an initial Gaussian random field, has shown that such alignments, expected naturally to occur in "top-down" scenarios, are also found in hierarchical clustering models of structure formation like the CDM. These results were corroborated with the use of high-resolution N-body simulations by West *et al*⁴¹, Splinter *et al*³⁶ and Onuora & Thomas²⁴. This fact has been explained as the result of an interesting property of Gaussian random fields that occurs for a wide range of initial conditions and which is the "cross-talk" between density fluctuations on different scales. This property is apparently also the cause of the observed filamentariness observed not only in "pancake" models but also in hierarchical models of structure formation; the strength of the effect, however, differs from model to model.

There is strong evidence that the brightest galaxy (BCGs) in clusters are aligned with the orientation of their parent cluster and even with the orientation of the large-scale filamentary structure within which they are embedded (cf. Struble³⁷, West⁴², Fuller, West & Bridges¹⁴). Furthermore, there is conflicting evidence regarding the alignment of cluster galaxies in general with the orientation of their parent cluster (cf. Djorgovski⁹, van Kampen & Rhee¹⁸, Trevese, Cirimele & Flin³⁹). It may be that general galaxy alignments may be present in forming, dynamically young, clusters, while in relaxed clusters violent and other relaxation processes

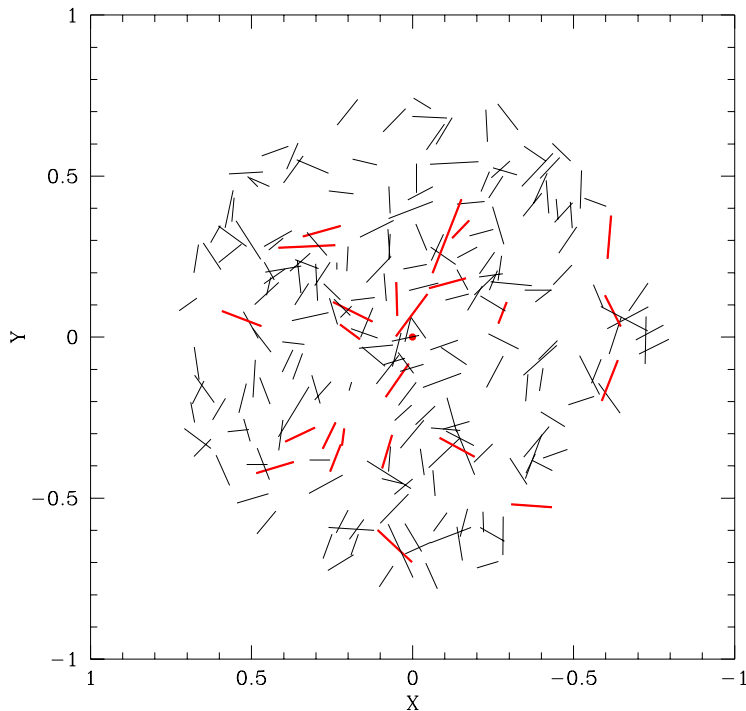


Figure 2: The distribution of galaxy position angles, within $0.75 h^{-1}$ Mpc, of A521. Position angles of galaxies with $m < m^*$ are shown in red. The alignment with the cluster position angle of $\theta \simeq 140^\circ$ is evident.

may erase such alignment features. Such seems to be the case of the Abell 85/87/89 complex (see Durret *et al*¹¹) and of Abell 521, a cluster at $z \simeq 0.25$ which is forming at the intersection of two filaments (Arnaud *et al*¹). Using wide-field CFHT imaging data of A521, Plionis *et al* (*in preparation*) have found statistical significant alignments not only of the predominantly bright but also of fainter galaxies with the major axis direction of the cluster (figure 2). It is interesting that this direction coincides with the direction of the nearest Abell cluster (see figure 3). Within the framework of hierarchical clustering, the anisotropic merger scenario of West⁴², in which clusters form by accreting material along the filamentary structure within which they are embedded, provides an interesting explanation of such alignments as well as of the observed strong alignment of BCGs with their parent cluster orientation. Evidence supporting this scenario was presented in West, Jones & Forman⁴³ in which they found, using Einstein data, that cluster substructures seem to be aligned with the orientation of their parent cluster and with the nearest-neighbouring cluster (see also Novikov *et al*²³). Such effect has been observed also in numerical simulations of cluster formation for a variety of power-spectra (van Haarlem & van de Weygaert¹⁷)

Tidal effects between protoclusters could be an alternative explanation of galaxy and cluster alignments in the popular hierarchical clustering scenario. However, a back of the envelope calculation shows that in order to have a fractional effect f on a test particle at a distance of $1 h^{-1}$ Mpc from a cluster of mass M_{cl} , caused by a perturber at a distance R , one needs a perturber mass of:

$$M_p \sim f R^3 M_c \quad (1)$$

Therefore for the typical intercluster nearest-neighbour separation of $\sim 18 h^{-1}$ Mpc, one would get a 5% effect for $M_p \sim 300 M_{cl}$! This however does not exclude the possibility that tides, produced by the cluster itself, could effect the shape and orientation of cluster members (see Barnes & Efstathiou² and Salvador-Sole & Solanes³¹ for thorough studies of tidal effects).

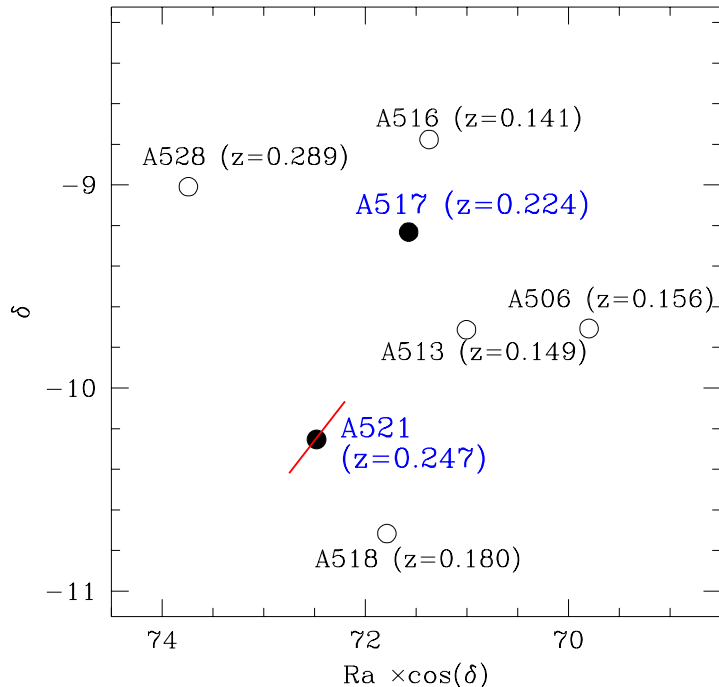


Figure 3: The large scale environment surrounding Abell 521. The major axis direction of A521 is pointing towards its nearest neighbour A517.

2 Methodology

Here I briefly present the methods used to determine the dynamical state of clusters, their shape, orientation and alignment.

2.1 Substructure Measure - Cluster Centroid Shift

Evrard *et al.*¹³ and Mohr *et al.*²² have suggested as an indicator of cluster substructure the shift of the center-of-mass position as a function of density threshold above which it is estimated. The *centroid-shift* (sc) is defined as the distance between the cluster center-of-mass, (x_o, y_o) , where $x_o = \sum x_i \rho_i / \sum \rho_i$, $y_o = \sum y_i \rho_i / \sum \rho_i$ and the highest cluster density-peak (x_p, y_p) , i.e.,

$$sc = \sqrt{(x_o - x_p)^2 + (y_o - y_p)^2}. \quad (2)$$

Notice here, that while the cluster center-of-mass changes as a function of density threshold, above which we define the cluster shape parameters, the position (x_p, y_p) remains unchanged. According to Kolokotronis *et al.*¹⁹, a large and significant value of sc is a clear indication of substructure.

The significance of such centroid variations to the presence of background contamination and random density fluctuations are quantified using Monte Carlo cluster simulations in which, by construction, there is no substructure. For each cluster a series of simulated clusters is produced having the same number of observed galaxies as well as a random distribution of background galaxies, determined by the distance of the cluster and the APM selection function. The simulated galaxy distribution follows a King-like profile:

$$\Sigma(r) \propto \left[1 + \left(\frac{r}{r_c} \right)^2 \right]^{-\alpha}, \quad (3)$$

where r_c is the core radius. We use the weighted, by the sample size, mean of most recent r_c and α determinations (cf. Girardi *et al.*^{15,16}), i.e., $r_c \simeq 0.085 h^{-1}$ Mpc and $\alpha \simeq 0.7$. We do test

the robustness of our results for a plausible range of these parameters (details can be found in Kolokotronis *et al*¹⁹). Naturally, we expect the simulated clusters to generate small sc 's and in any case insignificant shifts. Therefore, for each optical cluster, 1000 such Monte-Carlo clusters are generated and we derive $\langle sc \rangle_{\text{sim}}$ as a function of the same density thresholds as in the real cluster case. Then, within a search radius of $0.75 h^{-1}$ Mpc from the simulated highest cluster peak, we calculate the quantity:

$$\sigma = \frac{\langle sc \rangle_o - \langle sc \rangle_{\text{sim}}}{\sigma_{\text{sim}}}, \quad (4)$$

which is a measure of the significance of real centroid shifts as compared to the simulated, substructure-free clusters. Note that $\langle sc \rangle_o$ is the average, over three density thresholds, centroid shift for the real cluster.

2.2 Cluster Shape Parameters

To estimate the cluster parameters we use the familiar moments of inertia method (cf. Plionis, Barrow & Frenk²⁵); with $I_{11} = \sum w_i(r_i^2 - x_i^2)$, $I_{22} = \sum w_i(r_i^2 - y_i^2)$, $I_{12} = I_{21} = -\sum w_i x_i y_i$, where x_i and y_i are the Cartesian coordinates of the galaxies and w_i is their weight. We, then diagonalize the inertia tensor solving the basic equation:

$$\det(I_{ij} - \lambda^2 M_2) = 0, \quad (5)$$

where M_2 is the 2×2 unit matrix. The cluster ellipticity is given by $\epsilon = 1 - \frac{\lambda_2}{\lambda_1}$, where λ_i are the positive eigenvalues with ($\lambda_1 > \lambda_2$).

This method can be applied to the data using either the discrete or smoothed distribution of galaxies (for details see Basilakos, Plionis & Maddox³):

- *Method 1* ($w_i = 1$): Galaxies within an initial small radius around the cluster center of mass are used to define the initial value of the cluster shape parameters. Then, the next nearest galaxy is added to the initial group and the shape is recalculated. Finally we obtain the cluster shape parameters as a function of cluster-centric distance.
- *Method 2* ($w_i = \delta\rho/\rho$): This method is based on applying the moment of inertia procedure on the smoothed galaxy density distribution which we obtain using a Gaussian or other kernel on a grid.

Both methods have been found to provide consistent values of the cluster orientation but not so of the cluster ellipticity.

In order to test whether there is any significant bias and tendency of the position angles to cluster around particular values we estimate their Fourier transform:

$$C_n = \left(\frac{2}{N}\right)^{1/2} \sum_{i=1}^N \cos 2n\theta_i \quad (6)$$

$$S_n = \left(\frac{2}{N}\right)^{1/2} \sum_{i=1}^N \sin 2n\theta_i \quad (7)$$

If the cluster position angles, θ_i , are uniformly distributed between 0° and 180° , then both C_n and S_n have zero mean and unit standard deviation. Therefore large values (> 2.5) indicate significant deviation from isotropy.

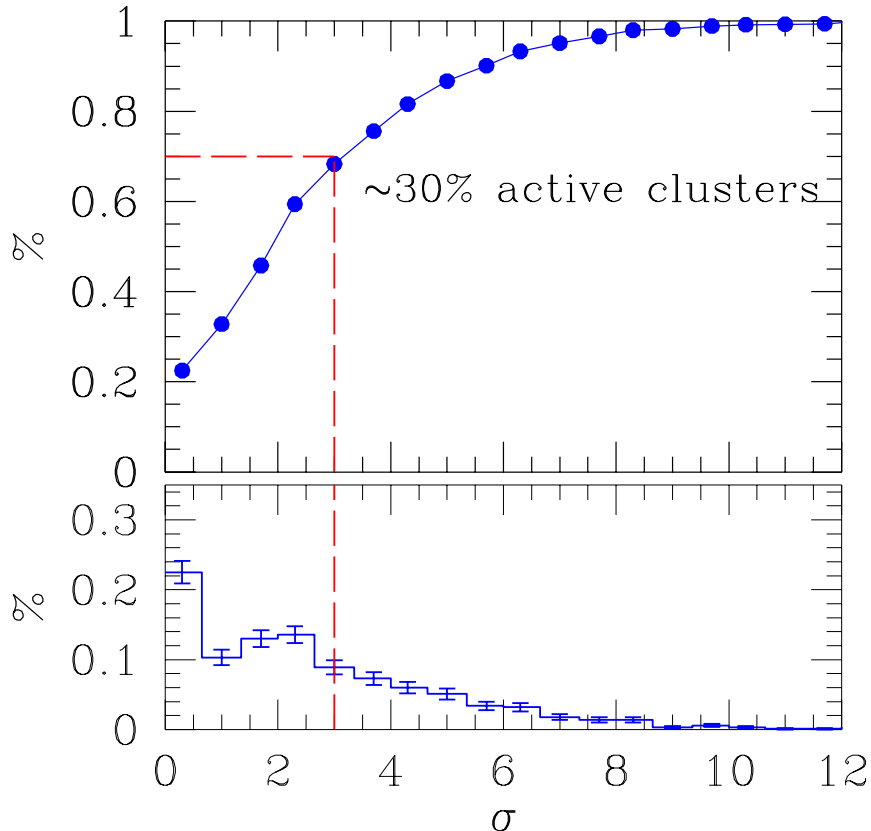


Figure 4: The fraction of clusters having substructure above the indicated significance level.

2.3 Alignment Measures

In order to investigate the alignment between cluster orientations, we define the relative position angle between cluster pairs by, $\phi_{i,j} \equiv |\theta_i - \theta_j|$. In an isotropic distribution we will have $\langle \phi_{i,j} \rangle \simeq 45^\circ$. A significant deviation from this would be an indication of an anisotropic distribution which can be quantified by (Struble & Peebles³⁸):

$$\delta = \sum_{i=1}^N \frac{\phi_{i,j}}{N} - 45 \quad (8)$$

In an isotropic distribution we have $\langle \delta \rangle \simeq 0$, while the standard deviation is given by $\sigma = 90/\sqrt{12N}$. A significantly negative value of δ would indicate alignment and a positive misalignment.

3 Results

3.1 Cluster substructure

Applying the above methodology to the ~ 900 APM clusters we find that about 30% of clusters have significant ($> 3\sigma$) substructure. In figure 4 we present the differential and cumulative distribution of clusters as a function of substructure significance. Note that defining as having significant substructure those clusters with $\sigma > 2$ or 2.5 increases the fraction to $\sim 50\%$ and 40% respectively. Furthermore, changing the parameters of the Monte-Carlo clusters changes the actual σ -values, although their relative significance rank-order remains unaltered. Our

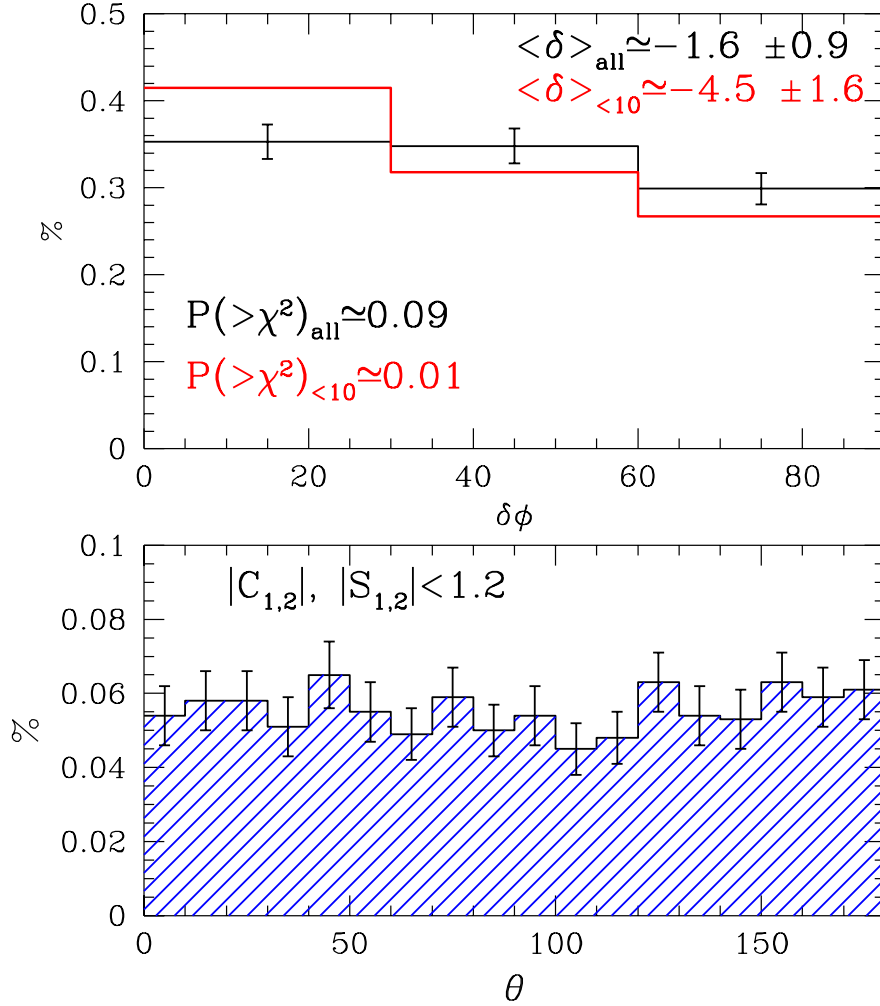


Figure 5: Upper panel: The distribution of relative position angles between nearest-neighbours. Lower panel: The distribution of APM cluster position angles.

results are in accordance with a similar study of the BCS and REFLEX clusters in which a considerable number of clusters do show indications of significant substructures (Schüecker *et al.*, in preparation).

3.2 Cluster Alignments

We have tested whether the well known nearest-neighbour alignment effect, present in the Abell clusters (cf. Bingelli 1982; Plionis 1994), is evident also in the poorer APM clusters.

A necessary prerequisite for this type of analysis is that there is no orientation bias in the distribution of estimated cluster position angles. In the lower panel of figure 5 we present the corresponding distribution for the APM clusters. It is evident that the distribution is isotropic, as it is also quantified by the Fourier analysis. In the upper-panel of figure 5 we present the distribution of relative position angles, $\delta\phi$, between APM nearest-neighbours for two separation limits (one for all separations and one for separations $< 10 h^{-1}$ Mpc). It is evident that there is significant indication of cluster alignments in the small separation limit.

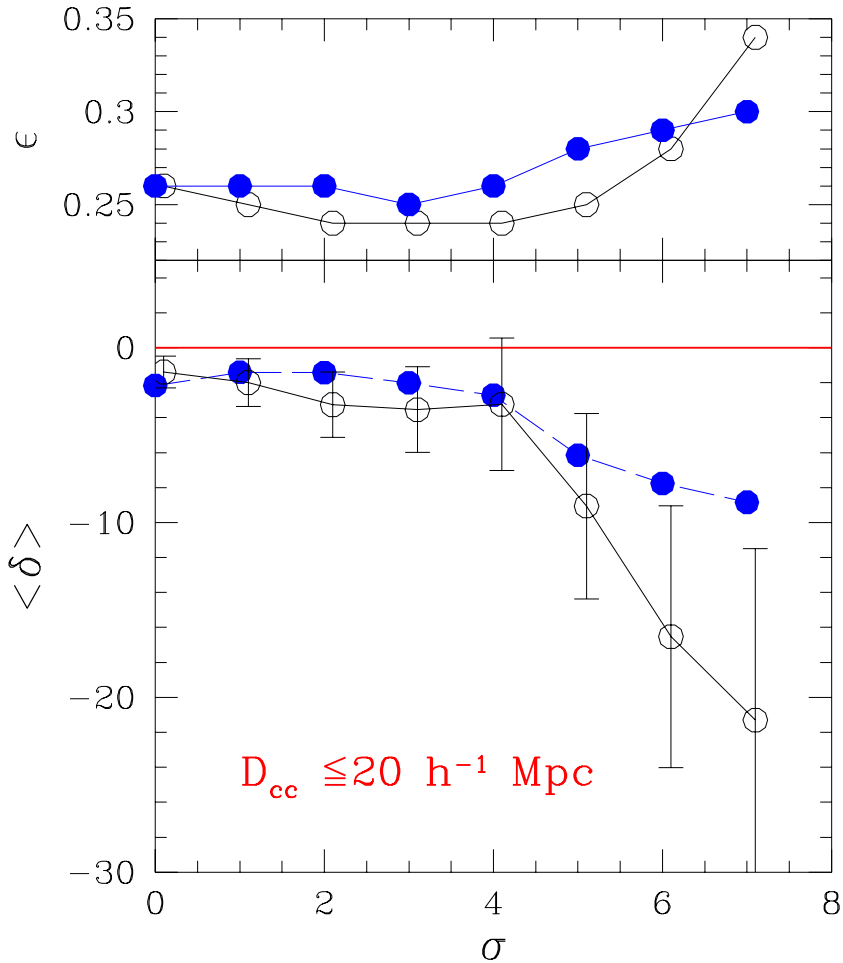


Figure 6: Lower panel: Alignment signal as a function of substructure significance level. Blue dots correspond to nearest-neighbours and white dots to all neighbours within $20 h^{-1} \text{ Mpc}$. Upper panel: The mean cluster ellipticity as a function of σ .

3.3 Cluster Alignments versus Substructure

We have correlated the alignment signal with the substructure significance indication in order to see whether there is any relation between the large-scale environment, in which the cluster distribution is embedded, and the internal cluster dynamics.

In the lower panel of figure 6 we present the alignment signal, $\langle \delta \rangle$, between cluster nearest-neighbours (blue dots) and between all pairs (open dots) with pair separations $< 20 h^{-1} \text{ Mpc}$. There is a strong correlation between the strength of the alignment signal and the substructure significance level. This result, based on the largest cluster sample available, supports the hierarchical clustering scenario and in particular the formation of cluster by anisotropic merging along the filamentary structure within which they are embedded (cf. West^{42,43}). This is supported also by the fact that the mean ellipticity of clusters increases as a function substructure significance level, which is in agreement with the flatness being a result of accreting substructures along a preferred direction.

If this view is correct then one would expect that clusters with significant substructure should be residing preferentially in high-density environments (superclusters), and this would then have an imprint in their spatial two-point correlation function. In the upper panel of figure 7 we present the spatial 2-point correlation function of all APM clusters (open dots) and of those with substructure significance $\sigma \geq 4$ (red dots). It is clear that the latter are significantly more

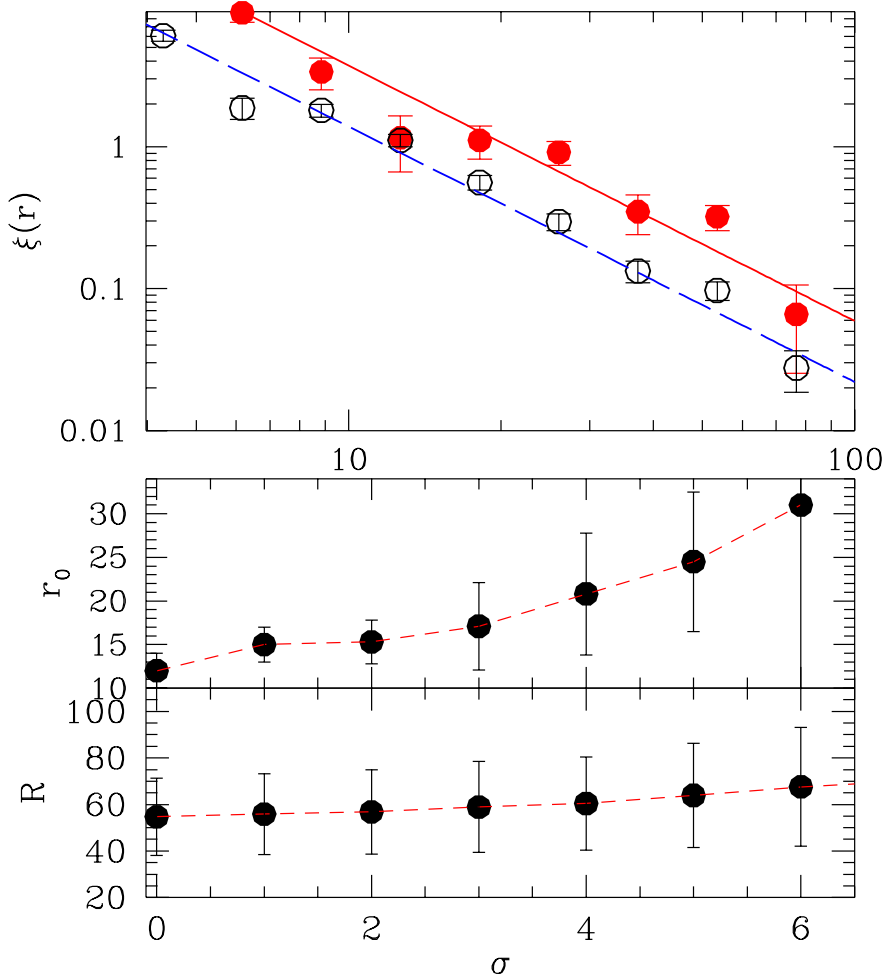


Figure 7: Upper panel: 2-point correlation function of all APM clusters (open dots) and of $\sigma > 4$ clusters. Lower panel: The cluster correlation length and the mean APM cluster richness as a function of substructure significance.

clustered. This can be seen also in the lower panel where we plot the correlation length, r_0 , as a function of σ , which is clearly an increasing function of cluster substructure significance level. To test whether this effect could be due to the well-known richness dependence of the correlation strength, we also present the mean APM richness as a function of σ and see that if any, there is only a small such richness trend. The conclusion of this correlation function analysis is that indeed the clusters showing evidence of dynamical activity reside in high-density environments, as anticipated from the alignment analysis. It is interesting that such environmental dependence has also been found for the cooling flow clusters with high mass accretion rates (Loken, Melott & Miller²¹).

3.4 Recent Evolution of Clusters ?

An interesting exercise is to see whether any of the previously discussed features show an evolution with redshift, since in a low-density (flat or not) universe we do not expect to see recent significant evolution of the structural or dynamical parameters of clusters. As a first such test we present in figure 8 the redshift dependence of the ellipticity for those clusters that show evidence of significant substructure ($\sigma \geq 6$). We find correlation coefficient $R \sim 0.3$ with probability

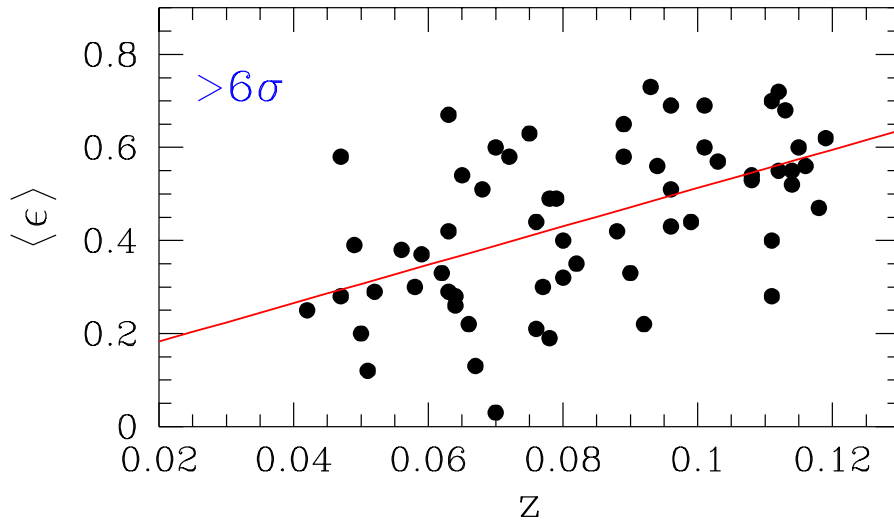


Figure 8: Evolution of cluster ellipticity with redshift for those APM clusters with very significant substructure.

of no correlation $P < 10^{-4}$. A similar trend is found for the whole APM sample but of lower correlation and significance. It is interesting that Plionis *et al.*²⁵ found a similar trend for Abell clusters using the Lick galaxy catalogue. If this result survives a thorough investigation of possible systematic effects then it would be interesting to compare this observable with N-body simulations of different cosmological models in an attempt to constrain the models.

4 Conclusions

We have presented evidence, based on the large APM cluster sample, that there is a strong link between the dynamical state of clusters and their large-scale environment. Clusters showing evidence of dynamical youth are significantly more aligned with their nearest neighbours and they are also much more spatially clustered. This supports the hierarchical clustering models and in particular the anisotropic merger scenario of West⁴².

Acknowledgments

I thank all my collaborators for allowing me to present our results prior to publication.

References

1. Arnaud, M., Maurogordato, S., Slezak, E., Rho, J., 2000, A&A, 355, 848
2. Barnes, J., Efstathiou, G., 1987, ApJ, 319, 575
3. Basilakos S., Plionis M., Maddox S. J., 2000, MNRAS, 315, 779
4. Bingelli B., 1982, AA, 250, 432
5. Bond, J.R., 1986, in *Galaxy Distances and Deviations from the Hubble Flow*, eds. Madore, B.F., Tully, R.B., (Dordrecht: Reidel), p.255
6. Bond, J.R., 1987, in *Nearly Normal Galaxies*, ed. Faber, S., (New York: Springer-Verlag), p.388 (Dordrecht: Reidel), p.255
7. Borgani, S. & Guzzo, L., 2001, Nature, 409, 39
8. Böhringer H., 1995, in Proceedings of the 17th Texas Symposium on Relativistic Astrophysics and Cosmology, eds. Böhringer H., Trümper J., Morfill G. E., The New York

Academy of Sciences

9. Djorgovski, S., 1983, ApJ, 274, L7
10. Dalton G. B., Maddox S. J., Sutherland W. J., Efstathiou G., 1997, MNRAS, 289, 263
11. Durret, F., Forman, W., Gerbal, D., Jones, C., Vikhlinin, A., 1998, A&A, 335, 41
12. de Grandi S., Molendi S., 1999, ApJ, 527, L25
13. Evrard A.E., Mohr J.J., Fabricant D.G., Geller M.J., 1993, ApJ, 419, L9
14. Fuller, T.M., West, M.J. & Bridges, T.J., 1999, ApJ, 519, 22
15. Girardi M., Biviano A., Giuricin G., Mardirossian F., Mezzetti M., 1995, ApJ, 438, 527
16. Girardi M., Giuricin G., Mardirossian F., Mezzetti M., Boschini W., 1998, ApJ, 505, 74
17. van Haarlem, M., van de Weygaert, R., 1993, ApJ, 418, 544
18. Kampen van E., Rhee, G.F.R.N., 1990, A&A, 237, 283
19. Kolokotronis, V., Basilakos, S., Plionis, M., Georgantopoulos, I., 2001, MNRAS, 320, 49
20. Lacey, C., Cole, S., 1996, MNRAS, 262, 627
21. Loken, C., Melott, A.L., Miller, C.J., 1999, ApJ, 520, L5
22. Mohr, J.J., Evrard, A.E., Fabricant, D.G., Geller, M.J., 1995, ApJ, 447, 8
23. Novikov, D. *et al.*, 1999, MNRAS, 304, L5
24. Onuora, L.I., Thomas, P.A, 2000, MNRAS, 319, 614
25. Plionis, M., Barrow, J.D., Frenk, C.S., 1991, MNRAS, 249, 662
26. Plionis M., 1994, ApJS., 95, 401
27. Richstone, D., Loeb, A., Turner, E.L., 1992, ApJ, 393, 477
28. Rizza E., Burns J. O., Ledlow M. J., Owen F. N., Voges, W., Blito M., 1998, MNRAS, 301, 328
29. Roettiger, K., Burns, J. & Loken, C., 1993, ApJ, 407, L53
30. Roettiger, K., Stone, J.M., Burns, J., 1999, ApJ, 518, 594
31. Salvador-Sole, E. & Solanes, J.M., 1993, ApJ, 417, 427
32. Sarazin, C.L., 1988, in *X-ray Emission from Clusters of Galaxies*, Cambridge Astrophysics Series, Cambridge Univ. Press.
33. Sarazin, C.L., 2001, in *Merging Processes in clusters of Galaxies*, eds. Feretti, L., Gioia, M., Giovannini, G., (Dordrecht: Kluwer).
34. Schindler S., 1999, in Giovanelli F., Sabau-Graziati L. (eds.), proceedings of the Vulcano Workshop 1999, *Multifrequency Behaviour of High Energy Cosmic Sources*, astro-ph/9909042.
35. Schindler S., 2000, in Giovanelli F., G. Mannocchi (eds.), proceedings of the Vulcano Workshop 2000, *Frontier Objects in Astrophysics and Particle Physics*, astro-ph/0010319.
36. Splinter, R.J., Melott, A.L., Linn, A.M., Buck, C., Tinker, J., 1997, ApJ, 479, 632
37. Struble, M.F., 1990, AJ, 99, 743
38. Struble, M.F., Peebles, P.J.E., 1985, AJ, 90, 582
39. Trevese, D., Cirimele, G., Flin, P., 1992, AJ, 104, 935
40. West, M. J., 1989, ApJ, 347, 610
41. West, M. J., Villumsen, J.V., Dekel, A., 1991, ApJ, 369, 287
42. West, M. J., 1994, MNRAS, 268, 79
43. West, M. J., Jones C., Forman W., 1995, ApJ, 451, L5
44. Zabludoff, A.I. & Zaritsky, D., 1995, ApJ, 447, L21